The Plant Cell, Vol. 2, 1039–1049, November 1990 © 1990 American Society of Plant Physiologists

# *Bronze-2* Gene of Maize: Reconstruction of a Wild-Type Allele and Analysis of Transcription and Splicing

**Juliana Nash,[1] Kenneth R. Luehrsen, and Virginia Walbot**

Department of Biological Sciences, Stanford University, Stanford, California 94305–5020

**The maize *Bronze-2* (*Bz2*) gene, whose product acts late in the anthocyanin biosynthetic pathway, has been cloned and its transcript has been mapped. We have developed a general procedure for reconstructing wild-type alleles from transposable element-induced mutants. An existing transposon-containing clone, *bz2::mu1* [McLaughlin, M., and Walbot, V. (1987). Genetics 117, 771–776], was modified by replacing the region of *bz2::mu1* containing the transposon with the corresponding polymerase chain reaction-amplified sequence from the progenitor allele that has no *Mu* insertion. Particle gun delivery of the reconstructed *Bz2* gene to embryonic scutellar tissue lacking a functional *Bz2* gene complemented the *bz2* mutant phenotype, as demonstrated by the production of purple spots. Having cloned the wild-type allele, we then analyzed the *Bz2* transcript, whose features include an 82-nucleotide 5′-untranslated leader, one small intron (78 base pairs) within the coding region, and multiple polyadenylation sites. Four *Mutator* transposon insertions that eliminate gene function were mapped within the 850-nucleotide transcription unit. We found that variable levels of unspliced *Bz2* RNA are present in purple husk tissue; this finding may indicate that the expression of *Bz2* is regulated in part at the level of transcript processing.**

## INTRODUCTION

Transposon tagging permits direct identification of genes responsible for biologically interesting phenotypes. In addition, the transposon tag allows recovery of genes that are difficult to clone by conventional methods, including developmental and regulatory loci and other genes whose products are not biochemically defined (Schmidt et al., 1987; McCarty et al., 1989). For instance, many structural and regulatory loci of the anthocyanin pathway have been characterized genetically by transposon mutagenesis and subsequently cloned by sequence homology to the insertion elements (for review, see Fedoroff, 1989). Because only mutant alleles containing the transposon can be cloned by this method, recovery of the progenitor allele traditionally has required the production and screening of either a cDNA library or a second genomic library prepared from the wild-type genotype. We demonstrated that progenitor alleles can be reconstructed readily by using polymerase chain reaction (PCR) to amplify the region of the progenitor that spans the transposon insertion and then substituting this region for the corresponding transposon-containing region of the cloned mutable allele. It is important to verify the restoration of function of such a reconstructed product; this is achieved most simply for an easily scorable phenotype such as anthocyanin pigmentation by showing that color is restored to mutant tissue upon delivery of the cloned gene.

[1] To whom correspondence should be addressed.

Many recessive mutants of anthocyanin pigmentation have been identified; for instance, mutations at the *Bronze-2* (*Bz2*) locus disrupt the production of the purple anthocyanin pigment and result instead in the accumulation of a bronze-colored pigment. *Bz2* was the last putative structural gene of the biosynthetic pathway to be identified genetically, and the gene product is proposed to catalyze the final step of pigment synthesis (Coe and Neuffer, 1988). The function of the *Bz2* product is unknown, but elucidation of the coding region of the gene may allow identification of the protein function. This laboratory used transposon mutagenesis to tag the *Bz2* gene, and four alleles of *Bz2* were found into which a *Mutator* (*Mu*) transposable element had inserted. As shown in Figure 1A, each of the four mutable alleles produced the same phenotype: small, purple (*Bz2*) sectors of revertant tissue on a bronze background (*bz2*); all four map within a 700-nucleotide (nt) region included in the 850-nt transcription unit (Figure 1B). One of these mutable alleles, *bz2::mu1*, was cloned by McLaughlin and Walbot (1987) by homology to *Mu1* and was verified to contain the *Bz2* gene by differential hybridization to RNA from green (the deletion mutant, *Δan1bz2*) and purple (*Bz2*) husk tissue. One polyadenylated 850-nt transcript was detected using an internal fragment of the *Bz2* sequence as a probe on RNA gel blots. The *Bz2* locus has also been tagged by a *Dissociation* element and subsequently cloned (Theres et al., 1987). Two cDNA clones isolated by this group suggested that transcription may

proceed in a direction opposite to that which would be consistent with the 850-nt transcript that we detected. Theres et al. (1988) also reported that these partial cDNA clones correspond to the 5′ region of the *Bz2* locus (orientation as in our gene model). Because they found this region of the gene to be partially homologous to unrelated sequences in the maize genome, it is possible that these antisense transcripts are not encoded by the *Bz2* gene region (Theres et al., 1988).

These ambiguities suggested that a more detailed examination of the molecular structure of the *Bz2* gene was required. Therefore, we reconstructed the progenitor *Bz2* allele using PCR technology, and confirmed the identity of the clone by delivering the reconstructed product to mutant *bz2* tissue with microprojectile bombardment to assay for complementation. Because the function of the *Bz2* gene product is unknown, we have searched for clues to its probable action in the *Bz2* gene structure and its nucleotide and predicted protein sequence. To define the transcription unit of *Bz2*, we used RNase protection and primer extension analyses, thereby enabling us to establish a transcription start site and map the position of one centrally located intron. These data further support our model for the gene organization of *Bz2*. We have also found that the splicing efficiency of the centrally located *Bz2* intron varies; the implications of this effect will be discussed.

## RESULTS

### *Cloning Strategy*

A detailed examination of *Bz2* gene regulation and function first required isolation of the wild-type gene. Previously, the mutable allele *bz2::mu1* was cloned, and the disruption of *Bz2* function was ascribed to a 1.4-kb *Mu1* insertion near the 3′ end of the gene (McLaughlin and Walbot, 1987). In *bz2::mu1* plants, proper *Bz2* gene function is restored to tissues upon excision of the *Mu1* element from the *bz2::mu1* allele, as demonstrated by the purple revertant spots in the aleurone tissue of *bz2::mu1* kernels shown in Figure 1A. We wanted to remove the *Mu1* insertion from the cloned *bz2::mu1* allele to create a cloned *Bz2* allele, but it is not possible to cause a *Mu1* excision event from a cloned allele. Because the *Mu1* insertion is contained within a unique Eco47III-BglII fragment in the *Bz2* gene, however, the *Mu1*-containing fragment could be removed and replaced with the corresponding region of the wild-type *Bz2* gene, as shown in Figure 2.

PCR amplification was used to produce about 500 ng of a 316-bp fragment of the *Bz2* allele that includes the entire Eco47III-BglII fragment lacking the *Mu1* insertion. Two rounds of amplification were necessary to generate enough DNA for the subsequent cloning step and to enhance the specificity of the PCR reaction. In the nested primer reactions, the PCR primers used in the second round hybridized to regions of the *Bz2* gene that were internal to the fragment produced by the primers used in the first round (Figure 2). A cloned *Bz2* allele, pBz2, was readily reconstructed by replacing the *Mu1*-containing Eco47III-BglII fragment of the mutable *bz2::mu1* allele with the amplified Eco47III-BglII product from the wild-type *Bz2* allele (Figure 2). Because of the infidelity of the Taq DNA polymerase used in the amplification reactions (Tindall and Kunkel, 1988), it was imperative to demonstrate the functionality of such a reconstructed allele and to analyze the sequence of the resulting clone.

### Expression of pBz2 in Transformed Tissue

To test whether pBz2 encodes a functional *Bz2* product, the cloned DNA was introduced by particle gun bombard-

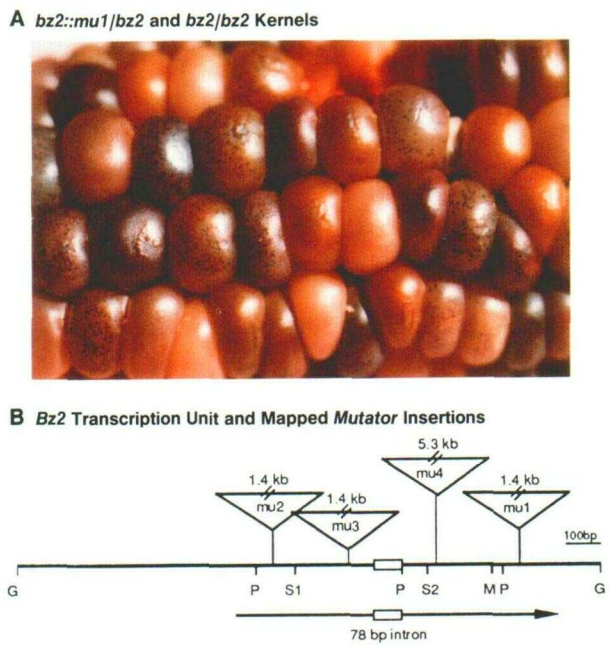


**Figure 1.** Map of the *Bz2* Region Showing Locations of *Mutator* Insertions within the 850-nt Transcription Unit.

**(A)** *bz2::mu1* kernels show the spotted phenotype in the aleurone characteristic of all four mutable alleles of the *Bz2* locus diagrammed in **(B)**.

**(B)** Insertions in *bz2::mu1*, *bz2::mu2*, and *bz2::mu3* are 1.4-kb *Mutator* elements (Barker et al., 1984), whereas *bz2::mu4* is a novel element (C.A. Warren and V. Walbot, unpublished data). The insertion site of *bz2::mu1* was determined by sequence analysis, as shown in Figure 4, and the other three insertions were mapped by restriction analysis and DNA hybridization with a 50-bp resolution.

G, BglII; P, PstI; S1, SstI; S2, SstII; M, MluI.

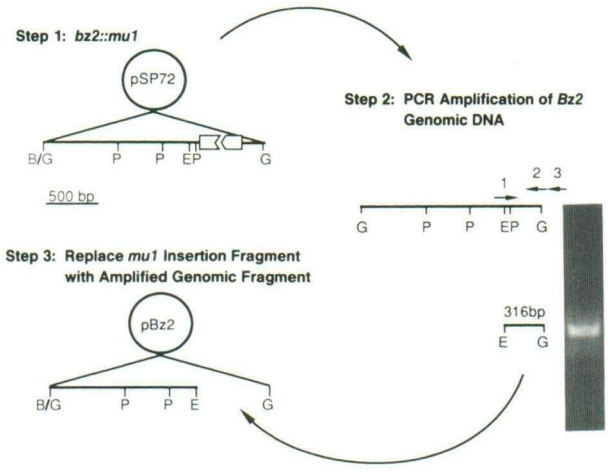


**Figure 2.** Reconstruction of a Wild-Type *Bz2* Allele from the Cloned Mutable Allele *bz2::mu1* Using Polymerase Chain Reaction.

The presumptive *Bz2* coding region of the *bz2::mu1* allele is interrupted by a 1.4-kb *Mutator* insertion element, designated by the broken open box (McLaughlin and Walbot, 1987).
**(Step 1)** The *bz2::mu1* allele, contained within a 5.2-kb BglII fragment, was ligated into the BamHI and BglII sites of pSP72. Clones were selected in which the BglII site upstream of the gene was destroyed in the BamHI/BglII fusion site.
**(Step 2)** The unique Eco47III-BglII fragment of the *Bz2* sequence was produced in two sequential rounds of amplification of genomic DNA from the wild-type *Bz2* genotype (B139). The first round of primers (primer 1 and primer 3 above) resulted in amplification of a 338-bp fragment of DNA, whereas the set of primers used in the second round of amplification (primer 1 and primer 2 above) enriched for the desired 316-bp product. This product included both the Eco47III and BglII cloning sites. Digested products of the second amplification were separated on a 2% agarose gel, as shown.
**(Step 3)** The unique Eco47III-BglII fragment of the *bz2::mu1* sequence including the entire *Mu* element was excised from the clone and replaced by the amplified region of the *Bz2* locus.
B, BamHI; G, BglII; P, PstI; E, Eco47III.

ment into recessive *bz2* scutellar tissue to assay for complementation of the mutant phenotype. The purple spots in Figure 3 indicate that host tissue has received and expressed pBz2, restoring the purple anthocyanin phenotype; this finding demonstrates that transposon mutagenesis with *Mutator* did, indeed, tag the *Bz2* locus. On a single embryo there were up to 50 spots, each of which probably represents a single delivery event, although the cells of the scutellum were so irregular that we could not determine the exact cell number of an individual spot as development proceeded. The genetic description of *R* alleles (Coe and Neuffer, 1988) predicts that scutellar tissue will be competent for the production of anthocyanin in the

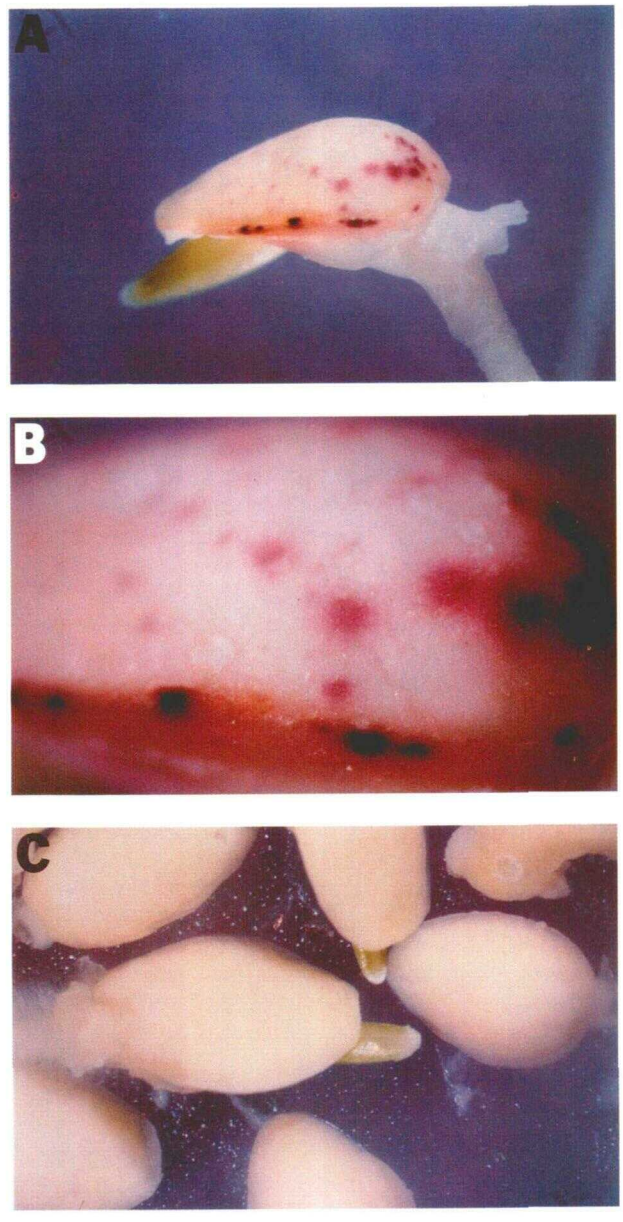


**Figure 3.** Complementation of *bz2 Rsc* Scutellar Tissue with pBz2.

**(A)** and **(B)** pBz2 DNA delivered to *bz2 Rsc* embryos (18 days after pollination) provided a functional *Bz2* enzyme, resulting in the synthesis of anthocyanin in target scutellar cells. Purple spots were observed 30 hr after bombardment.
**(C)** *bz2* embryos were bombarded with control plasmid pSPT673.

presence of the *Rsc* allele but not the *R* allele; the anthocyanin biosynthetic genes *A1* and *Bz1* have been demonstrated to be correctly controlled by the regulatory environment of the host tissue after particle gun delivery (Klein et al., 1989). Similarly, the presence of purple spots in *bz2 Rsc* tissue but not *bz2 R* tissue (data not shown) indicated that the introduced pBz2 was subject to the same regulatory controls as was the endogenous *Bz2* allele in the embryonic scutellum.

### *Bz2* Sequence

The sequence of the reconstructed clone pBz2 is displayed in Figure 4 and is identical to the corresponding *bz2::mu1* sequence except that the *Mu1* element and the 9-bp host duplication characteristic of *Mutator* insertions have been eliminated (Walbot et al., 1988). Typical of monocot gene structure, the relative GC content of *Bz2* exons/intron is 70%/55%; this feature may be important for intron recognition by the spliceosome (Goodall and Filipowicz, 1989). By computer analysis, we found a single open reading frame in the 850-nt transcript that encoded a 26-kD protein. No clues to the function of the *Bz2* gene product were obtained in a search through the GenBank, EMBL, and VecBase nucleotide sequence files because the *Bz2* sequence has no homology to any currently submitted gene sequences. Nor is there any striking similarity between the upstream regions of *Bz2* and other structural genes of the anthocyanin pathway in maize, despite the genetic and molecular evidence that some of these loci are responsive to the same regulatory signals (Coe and Neuffer, 1988; Chandler et al., 1989; Taylor and Briggs, 1990). This result is not surprising because the proposed consensus binding sites for regulatory proteins are fairly degenerate in the promoters of the anthocyanin structural genes (Goff et al., 1990).

### Identification of the Transcription Unit

Having a cloned functional allele of *Bz2* enabled us to analyze various aspects of the native *Bz2* transcript. First, we addressed the question of transcription initiation by primer extension analysis. As shown in Figure 5, four extended products were detected at positions −140 nt, +1 nt (labeled as transcription start), +66 nt, and +75 nt. The strongest signal was the +1 extended product corresponding to a 5′-untranslated leader of 82 nt relative to the second of the two in-frame ATGs in the *Bz2* sequence. The second ATG was used as the putative translation start site because it had a sequence context (ACCATGC) most closely resembling the consensus for maize translation start sites (Joshi, 1987a).

The −140 nt, +66 nt, and +75 nt extended products could not be confirmed by RNase protection analysis. RNA was isolated from two lines of purple *Bz2* plants, W23 and B139. The higher levels of *Bz2* RNA in the W23 line facilitated the analysis, although the results were always corroborated with B139 RNA; the B139 line was the source of the cloned *Bz2* gene and all the subsequent probes used in the analysis. As shown in Figure 6, a labeled antisense probe, corresponding to the 430-bp PstI

```
     BglII
1    AGATCTCATGACGGTGGATTGCAGAAACAGGACTAGAGAGTAAAGTGTACACCTTTGTGCAGAGTTTAAA
71   AACCTATTAGAATAGTCCATGTCCACGGATATGGACGAGTCATGGCTTAGATTTGATAATTAGTGTTTTG
141  TTTTCCAAAAATATTTTTGAAAAGTGGTTTTGAAAGGTCCGGCGGTTGAGCCGTGAGCTATGGTGGATGA
211  GAAGTCCAGTAGCTGCCTTTTTTTAAATGAAAATTGGTGAGAAACTACCAAGACACCTCGATGCGTGATT
281  GTTTGGCCAGGCAAGTCTGCTGGAGTCATAACCAAGCCAGCACTTACATTGTGCAACTACATGATGCGGA
351  TATTCCCAAGAATGTCTTTTCAAGATTTGATAGAAAATGCCTATAGTATCTAAAAGAACGGGCGCATCAT
421  CGTAGCCGTACATAAACAATGTTATTACCAACACGTGCTGTTCTGCTCTCGTGTAATGTCCAGCTACAAG
491  CACGCGCGCGAGCCGAATTTGGACGCACCAGAATCAGTTAGCTCGCACCAACCCGCACGAGCACCGACCG
561  GTCAATGACACGACTCGCCAGTCGCCACTACCGGTTCCCGTTTAAATTGCCGGCCGCATCAAGCTGAGGG
                ↓ transcription start                                PstI
631  CTGAGGCAGAGAGGTGCCAACAGAAGTCACGTCGAGACCAGCCGGCCGGCCGGACTGCAGCTCGTCGTCG
701  TCGATGACGGCCGGGACCATGCGTGTGCTAGGCGGGGAGGTCAGCCCGTTCACGGCGCGGGCGCGTCTGG
                                  SstI
771  CGCTGGATCTGCGCGGCGTGGCGTACGAGCTCCTCGACGAGCCGCTGGGGCCCAAGAAAAGCGACAGGCT
841  CCTCGCTGCCAACCCCGTCTACGGGAAGATCCCCGTGCTGCTCCTCCCCGACGGCCGCGCCATATGCGAG
911  TCCGCAGTCATCGTCCAGTACATCGAGGACGTGGCGCGTGAAAGCGGCGGCGCCGAGGCTGGCAGCCTGC
                                                    5' splice site
981  TGCTCCCGGACGACCCCTACGAGCGCGCCATGCACCGCTTCTGGACCGCCTTCATCGACGACAAGGTGAG
                                                                   PstI
1051 CACCGAGCAGAGCACGGCAGCAAGTGTCTTTTCTTCAAGGTAACGTGCAACAAACTGCCGTGCCTTTCTG
     3' splice site                                                SstII
1121 CAGTTTTGGCCGGCGCTGGATGCCGTCTCCCTGGCGCCGACCCCGGGAGCACGCGCGCAGGCCGCGGAAG
1191 ACACCCGCGCCGCGCTGAGCCTCCTGGAGGAGGCGTTCAAGGACCGCAGCAACGGCAGGGCTTTCTTCTC
1261 CGGTGGCGACGCCGCCGCCAGGCCTCCTGGACCTGGCCCTCGGATGCTTCCTACCGGCGCTCAGGGCCTGC
                                        MluI                    Eco47III
1331 GAGCGGCTCCACGGCCTCTCACTCATCGACGCGTCCGCGACGCCGCTGCTGGACGGGTGGAGCCAGCGCT
                PstI                ↓bz2::mu1 insertion site
1401 TCGCCGCGCACCCTGCAGCCAAGCGCGTCCTGCCAGACACGGAGAAGGTGGTGCAGTTCACGAGGTTCCT
1471 CCAGGTCCAGGCACAGTTCAGGGTCCACGTGTCCTAAATGATTTAGCGTCTCCAAAAGATTGTCAAAATC
1541 TCCGTCTAAAGTCTGTTTTAGAAACTTAAATCACTTTCAGGATTCTCGGAAATTGAGAGAAAAATAAAAT
1611 AACTTTTCACTAATCTTCAGAAATCTAAGAGAATTTCAGTTTTCAAACTAGCTCTAAATGTGGTGGAGAG
          BglII
1681 AAGGAAAAAAAGATCT
```

**Figure 4.** Nucleotide Sequence of *Bz2*.

The sequence was determined from the cloned *bz2::mu1* allele (McLaughlin and Walbot, 1987) and from the reconstructed *Bz2* gene (Figure 2). The nucleotide at which transcription initiates is labeled with an arrow (position 637), as is the site of the *Mu1* insertion in *bz2::mu1* (position 1432). Underlined are two in-frame ATGs, two in-frame stop codons, and the 9 bp of host sequence at the *bz2::mu1* insertion site that became duplicated upon insertion of the *Mutator* element. The 78-bp intron is shown in italics. The sequence of the *Mu1* element contained within *bz2::mu1* was virtually identical to the previously published *Mu1* sequences (Barker et al., 1984; Chandler et al., 1988). Its sequence differed from *Mu1.4-B37* (for numbering, see Chandler et al., 1988) by a T-to-C change at position 265, an additional C between positions 648 and 649, and an additional G between positions 1115 and 1116. The C residues at positions 576, 591, and 613 were not observed.

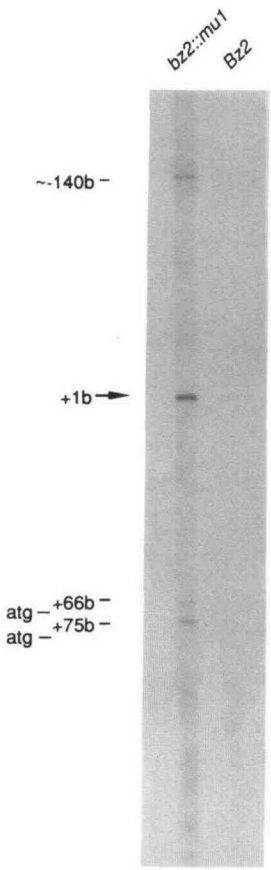


**Figure 5.** The *Bronze-2* Transcript Has an 82-nt 5′-Untranslated Leader.

Primer extension analysis was used to map the 5′ terminus of the *Bz2* mRNA. Poly $A^+$ RNA samples from *bz2::mu1* aleurone tissue (*bz2::mu1* lane) and from *Bz2* husk tissue (*Bz2* lane) were hybridized with the same primer to compare the effects of a downstream *Mu1* insertion on transcript initiation. Although less *Bz2* was expressed in husk than in aleurone tissues, the primary product (labeled +1 as the transcription start site) and all secondary products (−140 nt, +66 nt, and +75 nt relative to the transcription start site) were similar for both populations of RNA.

fragment P430 that spans the ATG, protected a hybrid RNA species of 430 bp (Figures 6B and 6C, P430 lanes). This finding indicated that the *Bz2* transcript must extend the full length of the probe; transcript initiation must be upstream of the 5′ PstI site, thus eliminating the +66 nt and +75 nt products as candidates for transcription initiation sites. Similarly, the +140 nt product cannot represent a transcription initiation site of *Bz2* because hybridization of W23 and B139 RNA with a probe extending 685 nt upstream of the PstI site GP685 (Figure 6A) protected no bands greater than 50 bp (data not shown). Therefore, transcription initiation must start within the 50-bp region upstream of the 5′ PstI site (position 687 in the sequence), a criterion met by only the most prominent of the primer extended products. We concluded that the strong band in the +1 position (50 bp upstream of the 5′ PstI site and 82 bp upstream of the second ATG) is the authentic start site for transcription.

To map the intron and 3′ end of the transcript by RNase protection, labeled antisense probes representing the full length of the *Bz2* gene were prepared and hybridized to total RNA from purple tissues (Figure 6A). The 245-bp and 60-bp bands protected by the intron-spanning SS390 probe demarcated a 78-bp intron internal to this probe region, whereas a 383-bp fragment was protected by unspliced transcripts (Figures 6B and 6C, SS390 lanes). For both the W23 and B139 alleles, the fragment of exon 2 protected by the SS390 probe appeared as three dominant bands as a result of RNase nibbling of the string of A:U base pairs at the 5′ end of the fragment (Figure 4, see 3′ splice site). Confirming the results with the SS390 probe, the P430 probe, which also includes the intron, yielded a 358-bp protected fragment for the spliced form of the transcript and a 430-bp band for the unspliced form (Figures 6B and 6C, P430 lanes). Both the SS390 and P430 probes indicated the presence of a single 78-bp intron; this intron contains the conserved 5′ and 3′ splice site consensus sites GT and AG, respectively, as labeled in Figure 4.

Consistent with our proposed model for the gene organization of *Bz2* in an 850-nt transcription unit, termination of transcription occurs downstream of the most 3′ PstI site of the gene (Figure 6A). The transcript is colinear with the coding region P300 probe representing the 300-bp PstI fragment, as demonstrated by protection of a 297-bp hybrid band (Figure 6B, P300 lane). In addition, RNase mapping with a 3′ end probe, MG340, suggested that there were three main regions for poly $A^+$ addition in the B139 allele (Figure 6C, MG340 lane). Higher plant genes in general use multiple poly $A^+$ addition sites, although there is no apparent consensus for a signal sequence required for adenylation (Joshi, 1987b). However, as shown in the MG340 lane, the largest band (255 nt) mapped to a position 10 nt downstream of a sequence identical to the conserved mammalian poly $A^+$ signal (AAUAAA) at position 1603 in the *Bz2* sequence (Figure 4). No consensus polyadenylation signal is found in the sequence represented by the other protected fragments. Also, the smallest and most intense bands protected by the MG340 probe were in the 150-nt region (position 1515 in the sequence). If these smaller bands represent authentic polyadenylation sites, the mRNAs terminate just 5 nt to 10 nt downstream of the first in-frame stop codon, UAA (see Figure 4), in an AU-rich region (10 nt of 11 nt are A or U). As we have shown (Figures 6B and 6C, SS390 lanes), such an AU-rich sequence can be hypersensitive to RNase digestion despite hybrid formation. It is also our opinion

## A RNase Protection of the *Bz2* Transcript

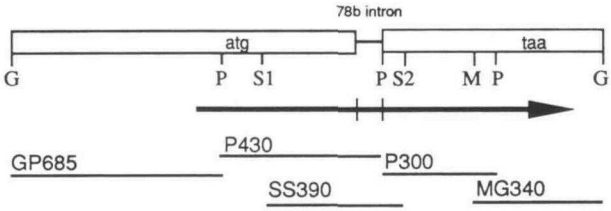


**Expected sizes of protected fragments**

| | P430 | SS390 | P300 | MG340 | GP685 |
|---|---|---|---|---|---|
| spliced | 358 nt | 245 + 60 nt | 297 nt | 260 nt | 49 nt |
| unspliced | 430 nt | 383 nt | 297 nt | 260 nt | 49 nt |

## B Protection of the W23 Allele of *Bz2*

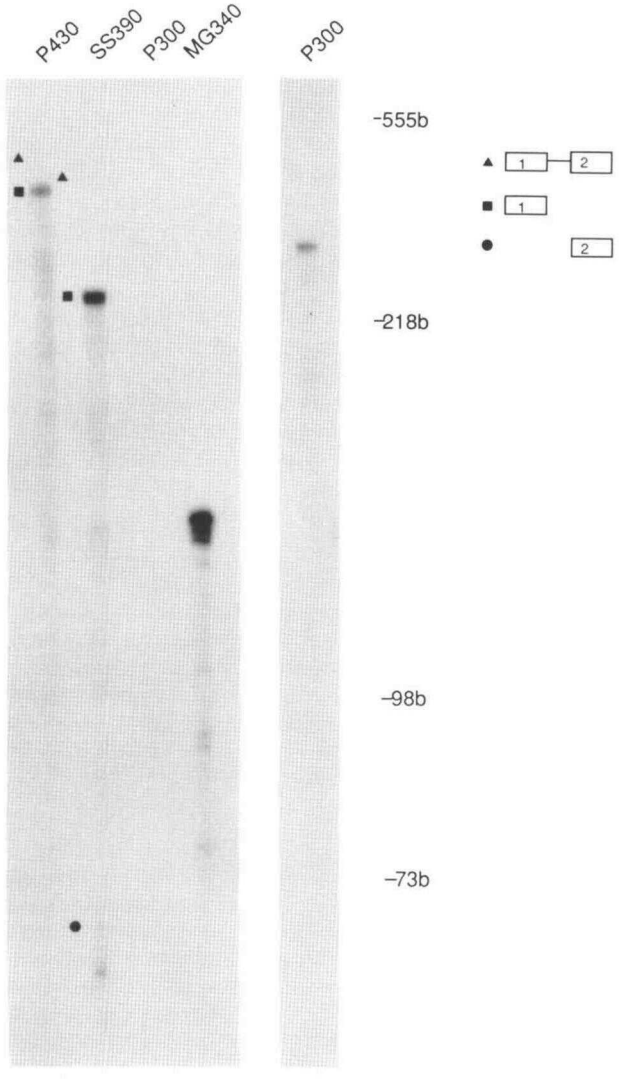


## C Protection of the B139 Allele of *Bz2*

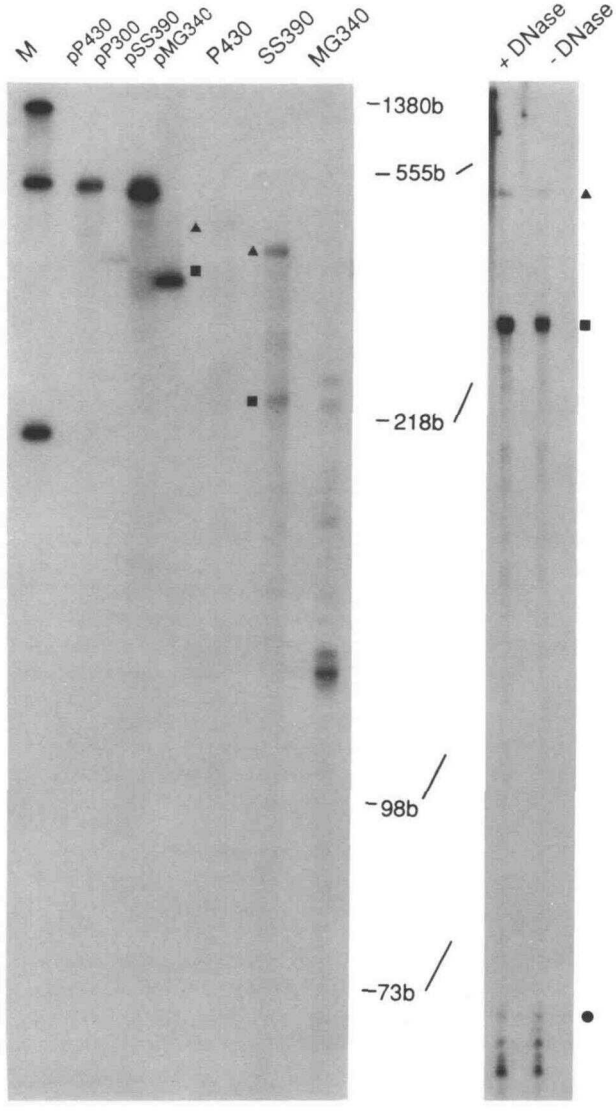


**Figure 6.** Mapping of the *Bz2* Transcript.

that poly $A^+$ addition in such close proximity to the stop codon is unlikely. Because the probes correspond to the sequence of the B139 allele, the inability of the MG340 probe to protect the 3′-untranslated region of the W23 allele may be the result of sequence divergence in this region of the allele. (The small bands in Figure 6B, MG340 lane, represent protection of transcript up to the translational termination site.) Except for the apparent divergence of the two alleles in the 3′-untranslated region, our probes from B139 (Robertson's *Mutator* line) fully protected both spliced and unspliced *Bz2* RNA of the W23 inbred in the coding region of the gene; we conclude that the two alleles are colinear for at least 80% of the full transcript length, from 20 bases upstream of the ATG through the PstI site at position 1415.

### mRNA Processing Effects

We found in our RNase protection analysis that more unspliced *Bz2* message accumulated in plants grown in our field than in plants grown in our greenhouse (compare the SS390 lane for greenhouse-grown plants in Figure 6B with the SS390 lane for field-grown plants in Figure 6C). Unspliced transcripts from the *Bz2* allele in the greenhouse-grown plants were present at approximately 10% of the level of spliced transcripts, whereas unspliced transcripts in field-grown plants represented up to 60% of the total *Bz2* mRNA. We confirmed that the full-length protected fragments were RNA::RNA hybrids and not the result of contaminating DNA in the samples by pretreating the RNA preparations with DNase (Figure 6C, +DNase and −DNase lanes). Because this discrepancy between splicing efficiencies was observed between two alleles in different genetic backgrounds (compare the SS390 lane for W23 plants in Figure 6B with the SS390 lane for B139 plants in Figure 6C), we then investigated the role of a potential genetic component on the splicing failure. No *cis* effect due to allelic divergence in the intron region was responsible for the differences in splicing of these two alleles; the intron and surrounding exon sequences of the W23 allele were sequenced following PCR amplification, and the sequences conformed identically to the B139 sequence (data not shown).

When plants of the B139 genotype were grown in the greenhouse and in the field, significant amounts of unspliced transcripts accumulated only in the field-grown tissue (Figure 6C, compare field-grown plants in the SS390 lane with greenhouse-grown plants in the +DNase and −DNase lanes). Therefore, this splicing effect was not conferred simply by the genetic background in which the allele resided. To show that the developmental age of the source tissue was not the major determinant of the accumulation of unspliced transcripts in field-grown plants, developmentally similar tissue was compared in the two growth conditions. Husk tissue harvested just before silking was demonstrated to accumulate approximately 60% unspliced message in field-grown tissue (Figure 6C, SS390 lane), whereas <10% unspliced message accumulated in greenhouse-grown tissue (Figure 6C, +DNase and −DNase lanes). Therefore, the presence of unspliced transcripts in our samples appeared to reflect an environmental effect (greenhouse versus field growth conditions) on the splicing efficiency of *Bz2*. Additional experiments are in progress to determine the cause of splicing failure; in particular, we are examining the effect of growth conditions on splicing efficiency. Unlike greenhouse conditions in which plants experience 30°C days and 25°C nights, field conditions in 1989 included temperature extremes of 10°C to 43°C.

---

**Figure 6.** (continued).

**(A)** The *Bz2* transcript was mapped by RNase protection; antisense RNA probes were synthesized from the *Bz2* gene fragments indicated, and the expected sizes of protected fragments with each probe are listed.

**(B)** RNA from the W23 line of maize (a deep purple plant, *B Pl*, with abundant *Bz2* mRNA) was protected by the two intron-spanning probes P430 (P430 lane) and SS390 (SS390 lane) and identifies the 78-bp intron diagrammed in **(A)**; protected fragments from spliced [exon 1 (■) and exon 2 (●)] and unspliced (▲) transcripts are indicated. The P300 and MG340 probes protect regions downstream of the P430 and SS390 probes. The P300 lane on the right is a longer exposure of the P300 lane on the left. The 3′ end probe, lane MG340, fails to protect the 3′-untranslated region of the *Bz2* allele in W23 tissue because the probe represents the sequence of the B139 *Bz2* allele [shown in **(C)**].

**(C)** RNA from the B139 line of maize (the pale purple progenitor line, *B pl*, with rare *Bz2* mRNA) was also protected by the P430 and SS390 probes (P430 and SS390 lanes), confirming the 78-bp intron. The fragment protected by the P300 probe is identical for both the W23 and B139 RNAs (data not shown for B139). The 3′ end probe, lane MG340, protects several fragments representing multiple transcript endpoints. The GP685 probe, a 753-nt sequence, does not hybridize with any detectable fragments of *Bz2*; the expected 50-nt protected fragment is too small to be resolved (data not shown).

To determine that the detected unspliced transcripts were the result of incomplete splicing of the 78-bp intron rather than DNA contamination, husk RNA from greenhouse-grown plants was treated with (+DNase lane) or without (−DNase lane) RNase-free DNase before RNase protection by the SS390 probe.

Labeled probes in like-labeled lanes were pP430, pP300, pSS390, and pMG340 of sizes 511 nt, 380 nt, 492 nt, and 351 nt, respectively, and were included as markers. Transcript RNAs from SP6 control templates (New England Biolabs) are in lane M.

In mutable alleles, transposable element insertions are known to be a source of disruption of the RNA processing of pre-mRNA. Strommer and Ortiz (1989) showed that *Mu1* insertion in the first intron of the *Adh1-S3034* allele caused severe effects on intron splicing by providing an alternative 5′ splice site that was recognized by the spliceosome machinery in the presence of the native mRNA 5′ splice site (Strommer and Ortiz, 1989). To determine whether the presence of a downstream *Mu1* insertion affects transcription initiation of the *Bz2* gene, we used RNA from *Bz2* plants (husk tissue) and *bz2::mu1* plants (aleurone tissue) in a primer extension analysis and found no qualitative differences in transcription initiation between these two alleles (Figure 5). This primer extension analysis also revealed no qualitative differences in transcription initiation at the *Bz2* gene in aleurone and husk tissue, indicating that transcription initiation is similar in these two tissue types (Figure 5).

## DISCUSSION

The use of transposon tagging to identify and ultimately to clone genes necessarily results in the recovery of a mutant allele when often it is the wild-type allele that is required to examine gene expression and function. We have developed a method utilizing PCR to reconstruct the wild-type *Bz2* allele from a cloned *bz2::mu1* allele. Our cloned *Bz2* gene includes the 850-bp transcription unit with 700 bp of upstream and 200 bp of downstream sequence. Particle gun delivery of the reconstructed *Bz2* clone to tissue lacking a functional *Bz2* enzyme restored anthocyanin expression to the host tissue. These techniques outline a rapid approach to a site-directed mutagenesis study of gene function. Modifications of the PCR protocol used here can amplify specific regions of a gene with base changes designated by substitutions in the PCR primer sequences. Using the particle gun, quick delivery of the mutagenized products to tissue that is recessive for the locus in question can determine the relative effect of the mutation on the function of the gene product by complementation assay. Because anthocyanin expression is a sensitive visual marker for gene function studies, it is now possible to determine the regions of the gene important for *Bz2* function and to analyze in more detail the promoter structure and regulatory features of the *Bz2* gene.

The organization of the *Bz2* gene is not unusual for a higher plant gene; the length of the 5′-untranslated leader (82 nt), a relatively small intron (78 bp), and the use of multiple polyadenylation sites are common characteristics. The protein coding region is GC rich (70% GC), as expected for monocot exons (Goodall and Filipowicz, 1989). Few genes have more than one translation start site, as *Bz2* does; an upstream ATG can depress the translational efficiency of a downstream ATG by competition for the translational machinery (Kozak, 1984). The two ATGs in *Bz2* are in frame; hence, translational initiation at the upstream start site is unlikely to have a negative regulatory effect on the production of the *Bz2* product, although the protein would be 5 amino acids longer.

Despite the lack of homology of the *Bz2* promoter region with the corresponding regions of other anthocyanin biosynthetic genes, genetic evidence suggests that *Bz2* is a structural gene that is coordinately regulated with other members of the pathway (Dooner, 1983). Because *Bz2* acts later than *Bz1*, as shown by precursor feeding experiments (Reddy and Coe, 1962), and the function of *Bz1* is to glycosylate anthocyanidins, we suggest that *Bz2* may further modify the cyanin-glycoside (product of *Bz1*) by the addition of a sugar residue or an acyl group such as malonic acid. Harborne (1986) identified malonated forms of anthocyanin in maize; this finding implies that an additional acylation step late in the anthocyanin pathway is required for combination of malonic acid with anthocyanin. The fact that these malonated forms are readily destroyed by the acid extraction routinely used in anthocyanin separation procedures may explain their relatively recent discovery (Harborne, 1986). Acylation of anthocyanins with malonic, malic, or succinic acid is found in many plants; this process occurs late in the pathway and could be a function provided by *Bz2* in maize.

In the absence of experimental evidence about the function of *Bz2*, our initial approach was to analyze the transcription and expression of *Bz2*. We observed that substantial unspliced *Bz2* transcripts accumulate in field-grown maize husk tissue. The processing of the *Bz2* intron is variable and appears to depend on the environmental circumstance in which the gene is expressed. There are several other instances in which unspliced mRNAs have been detected in plant tissues. Winter et al. (1988) detected unspliced *hsp70* mRNA in petunia leaves exposed to $CdCl_2$; only spliced mRNA was detected in heat-shocked leaves (Winter et al., 1988). In another stress treatment, Ortiz and Strommer (1990) detected unspliced *Adh1* mRNA in hypoxic maize seedlings; aerated seedlings had fully spliced transcript (Ortiz and Strommer, 1990). In addition, we detected substantial amounts of unspliced mRNA containing either intron 1 of maize *Adh1* or intron 3 of maize actin in electroporated maize protoplasts given a 10-min treatment at 45°C (K.R. Luehrsen, unpublished results); heat shock may increase the amount of unspliced mRNA from cellular genes and introduced genes in this system.

These three examples of the accumulation of unspliced mRNA in plant cells may reflect splicing failure during stress. In *Drosophila* cells, heat shock disrupts splicing of *hsp83*; unspliced transcripts are exported to the cytoplasm and are translated (Yost and Lindquist, 1988). The *Bz2* intron may be particularly sensitive to perturbations in the efficient functioning of the spliceosome because its size,

78 bp, approaches the minimal length required for accurate splicing in plants (Goodall and Filipowicz, 1990). Experiments are in progress to determine the cause(s) of the inefficient splicing of *Bz2* in field-grown plants and the impact of controlled stresses on splicing in *Bz2* and other pre-mRNAs. Unlike many animals, temperate zone plants and their cellular machinery are subjected daily to wide fluctuations of temperature. If splicing failure is a common result of thermal and heavy metal stress, then the accumulation of unspliced transcripts and dysfunctional proteins could present a continuous strain on the basic functioning of the organism. To survive, such plants may require especially effective mechanisms to tolerate the presence of unspliced transcripts and aberrant proteins that are produced during exposure to daily thermal stress.

## METHODS

### Plant Material

Seed stocks of the purple *Mutator* line B139 (our designation) obtained from D.S. Robertson (Robertson, 1978) contain all the genes required for anthocyanin biosynthesis. The original mutable *bz2::mu1* was isolated by P. McLaughlin and V. Walbot (McLaughlin and Walbot, 1987); all subsequent *bz2* mutable alleles are also derivatives of the B139 line. The *Rsc* allele is in a W23 background and carries the *bz2* allele identified by E.H. Coe, Jr. (Coe and Neuffer, 1988).

The nomenclature used for the mutant alleles (*bz2::mu1*, *bz2::mu2*, *bz2::mu3*, and *bz2::mu4*) indicates the mutant allele (*bz2*), type of insertion (*Mutator*), and the numerical order in which the mutant was isolated.

### DNA and RNA Isolation

DNA samples were extracted from etiolated maize seedlings germinated in the dark at 25°C for 6 days as described previously (Walbot and Warren, 1988). Samples were resuspended in 10 mM Tris-HCl, pH 8, 0.1 mM EDTA and treated with RNase A (Sigma) before use in the PCR reactions.

Total RNA was isolated from husk or aleurone (peeled from kernels with forceps) tissue from plants grown in the greenhouse or in the field. The tissue was immediately frozen in liquid nitrogen and homogenized to a fine powder with a mortar and pestle. RNA purification was as described (Logemann et al., 1987), except that the first centrifugation was eliminated. Selection of poly $A^+$ RNA was by affinity to Hybond mAP paper (Amersham Corp.), according to the manufacturer's instructions.

### Reconstruction of the *Bz2* Allele and Sequence Analysis

Previously, a fragment of maize DNA containing the *bz2::mu1* allele was cloned into the EcoRI and BglII sites of pUC18 (McLaughlin and Walbot, 1987). The BglII fragment containing the *bz2::mu1* region was then subcloned into the BamHI/BglII sites of pSP72 (Promega Biotec), which destroyed the BglII site positioned upstream of the transcription unit of the gene. The *Mu1* insertion of this allele is within an Eco47III-BglII fragment. This fragment was exchanged with a PCR-amplified copy of this region from the wild-type *Bz2* sequence to generate a reconstructed *Bz2* allele. Each PCR reaction utilized 400 ng of B139 maize DNA, 200 mM each deoxynucleotide triphosphate (Promega Biotec), and 0.05 units/$\mu$L Amplitaq (Perkin-Elmer Cetus) in an Ericomp Programmed Cycle Reactor. As shown in Figure 2, two rounds of amplification were run in which the 3′ primer for the second round paired with sequences internal to the products of the first round to enhance the specificity of the reaction. The sequence of the 5′ primer is 5′-GGAGCCAGCGCTTCGCCGCGCACCCTGCAGCC (primer 1 in Figure 2), and the sequences of the two 3′ primers are 5′-GATAGTAGCTAGTGAGATCTTTTTTTC (primer 2) and 5′-GGGCGATGACTTTTTAGACAA (primer 3). The reaction conditions were as suggested by the enzyme supplier, and the amplification consisted of 30 cycles of 1 min at 95°C, 1 min at 55°C, and 2 min at 74°C, followed by 5 cycles of 1 min at 74°C.

Both the *bz2::mu1* clone and the PCR-amplified product of *Bz2* DNA covering the region of the *Mu1* insertion were digested with Eco47III and BglII. The digested products were separated in a 1% NuSieve low melting point agarose gel. The 4-kb *bz2::mu1* fragment and the 316-bp amplified *Bz2* fragment were each cut out of the gel and melted, and 5-$\mu$L samples of each were mixed, ligated, and transformed into DH5$\alpha$ cells (Sambrook et al., 1989). Plasmid DNAs from the recombinant clones were isolated on CsCl density gradients, and the region of the clone into which the amplified product was inserted was sequenced using a Sequenase kit (United States Biochemical). Only one of five transformants had a perfect sequence based on comparison with the *bz2::mu1* sequence (Walbot et al., 1988); this clone is referred to as pBz2.

Fragments derived from the central BglII fragment of the cloned *bz2::mu1* allele (clone 15; McLaughlin and Walbot, 1987) were subcloned into mp19 or pBSKS(−) (Stratagene). Dideoxy sequencing was accomplished using standard protocols. The sequence of both strands of the *bz2* gene was determined; only one strand of the *Mu1* element was done.

### Particle Bombardment

For each test, 25 immature embryos harvested 18 days after pollination were plated with the scutellum side up on N6 medium supplemented with 20% sucrose and 1% agarose (Chu et al., 1976). The same day, 1.25 mg of 1.7-$\mu$m (average diameter) microprojectiles were coated with 7 $\mu$g of plasmid DNA by the addition of 2 mM spermidine and 50 mM $CaCl_2$ (Klein et al., 1988) and were delivered to maize tissue by gunpowder-fired high-velocity particle bombardment (Klein et al., 1987) using the facility at the University of California, Berkeley. The tissue was grown at 28°C in fluorescent light thereafter. pSPT673 (Promega Biotec) was used as the control plasmid in bombardment experiments.

### Primer Extension

One hundred nanograms of primer were end labeled with 50 $\mu$Ci of $\gamma$-$^{32}$P-ATP in kinase buffer (50 mM Tris-HCl, pH 7.2, 10 mM $MgCl_2$, 5 mM DTT, 0.1 mM spermidine, and 0.1 mM EDTA) and

5 units of T4 polynucleotide kinase (New England Biolabs) for 30 min at 37°C. About 5 μg of poly $A^+$ RNA were extended with the primer 5′-GTCGCTTTTCTTGGGCCC. The kinase was inactivated at 65°C for 5 min before purification of the labeled primer on a P10 (Bio-Rad) spin column. Labeled primer [$2 \times 10^5$ cpm (Cerenkov)] was annealed to heat-denatured poly $A^+$ RNA at 35°C for 10 min, followed by cDNA synthesis at 42°C for 1 hr with avian myeloblastosis virus reverse transcriptase (Seikagaku) in a buffer composed of 50 mM Tris-HCl, pH 8.3, 6 mM $MgCl_2$, 40 mM KCl, 1 mM each of all four deoxynucleotide triphosphates, 20 mM DTT, and 0.5 units/μL RNAsin (Promega Biotec). The extended products were ethanol precipitated and loaded on a 6% polyacrylamide sequencing gel; fragments were sized by migration relative to a DNA sequencing ladder.

### RNase Protection

Fragments of the cloned *bz2::mu1* allele were subcloned into the pBSKS(−) vector and phage RNA polymerases were used to produce antisense transcripts for use as probes in the RNase protection experiments. The 430-bp and 300-bp PstI fragments of the *bz2::mu1* allele were not disrupted by the *Mu1* insertion and could, therefore, be used as probes to the wild-type *Bz2* transcript. These fragments were ligated into the PstI site of pBSKS(−) to create pP430 and pP300, respectively. The 387-bp SstI-SstII intron-spanning fragment was cloned into the same sites of pBSKS(−) to produce pSS390, and the 687-bp BglII-PstI (5′-upstream region) fragment was inserted into the BamHI-PstI sites of the pBSKS(−) vector to generate pGP685. T3 or T7 RNA polymerase (New England Biolabs) was used for the appropriate constructs to incorporate $\alpha$-$^{32}$P-CTP in an in vitro transcription reaction according to standard protocols (Krieg and Melton, 1987). Antisense RNA probes of sizes 511 nt, 380 nt, 492 nt, and 753 nt were synthesized from pP430, pP300, pSS390, and pGP685, respectively. Digestion of pBz2 by MluI and subsequent RNA synthesis by T7 RNA polymerase produced a 351-nt antisense probe, MG340, corresponding to the 3′ end of the *Bz2* gene.

Labeled probe [$5 \times 10^5$ cpm (Cerenkov)] was hybridized to 15 μg of total cellular RNA at 45°C overnight for each protection assay as described (Luehrsen and Walbot, 1991). Samples were digested sequentially with RNase H (Bethesda Research Laboratories), followed by RNases A and T1. The protected fragments were treated with SDS and proteinase K (Bethesda Research Laboratories), extracted with phenol/$CHCl_3$, and ethanol precipitated. Treatment of RNA samples with RNase-free RQ1 DNase (Promega Biotec) where indicated was for 20 min at 37°C, and was completed before the hybridization step. RNA hybrids were denatured and the labeled fragments were separated on a 6% acrylamide gel. The gels were fixed with 10% methanol/10% acetic acid and autoradiographed with two intensifying screens for 0.5 day to 3 days.

## ACKNOWLEDGMENTS

We thank Chris Warren for the mapping data of the mutable alleles. Special thanks to Michael Freeling and Steven Ruzin for use of the particle gun facility at the University of California, Berkeley. J.N. was supported with a National Science Foundation predoctoral fellowship and K.R.L. by a postdoctoral fellowship from the American Cancer Society (PF 2943). Research was supported by Grant GM 32422 from the National Institutes of Health.

Received June 22, 1990; accepted August 20, 1990.

## REFERENCES

**Barker, R.F., Thompson, D.V., Talbot, D.R., Swanson, J., and Bennetzen, J.** (1984). Nucleotide sequence of the maize transposable element *Mu1*. Nucl. Acids Res. **12,** 5955–5967.

**Chandler, V.L., Talbert, L.E., and Raymond, F.** (1988). Sequence, genomic distribution and DNA modification of a *Mu1* element from non-*Mutator* maize stocks. Genetics **119,** 951–958.

**Chandler, V.L., Radicella, J.P., Robbins, T.P., Chen, J., and Turks, D.** (1989). Two regulatory genes of the maize anthocyanin pathway are homologous: Isolation of *B* utilizing *R* genomic sequences. Plant Cell **1,** 1175–1183.

**Chu, C.C., Sun, C., Yin, K.C., Chu, C.Y., and Bi, F.Y.** (1976). Establishment of an efficient medium for another anther culture of rice through a comparative experiment of the nitrogen sources. Sci. Sinica **18,** 659–668.

**Coe, E.H., Jr., and Neuffer, M.G.** (1988). The genetics of corn. In Corn and Corn Improvement, 3rd ed, G.F. Sprague and J.W. Dudley, eds (Madison, WI: American Society of Agronomy), pp. 81–258.

**Dooner, H.K.** (1983). Coordinate genetic regulation of flavonoid biosynthetic enzymes in maize. Mol. Gen. Genet. **189,** 136–141.

**Fedoroff, N.V.** (1989). Maize transposable elements. In Mobile DNA, D.E. Berg and M.M. Howe, eds (Washington, DC: American Society for Microbiology), pp. 375–411.

**Goff, S.A., Klein, T.M., Roth, B.A., Fromm, M.E., Cone, K.C., Radicella, J.P., and Chandler, V.L.** (1990). Transactivation of anthocyanin biosynthetic genes following transfer of *B* regulatory genes into maize tissues. EMBO J. **9,** 2517–2522.

**Goodall, G.J., and Filipowicz, W.** (1989). The AU-rich sequences present in the introns of plant nuclear pre-mRNAs are required for splicing. Cell **58,** 473–483.

**Goodall, G.J., and Filipowicz, W.** (1990). The minimum functional length of pre-mRNA introns in monocots and dicots. Plant Mol. Biol. **14,** 727–733.

**Harborne, J.B.** (1986). The natural distribution in angiosperms of anthocyanins acylated with aliphatic dicarboxylic acids. Phytochemistry **25,** 1887–1894.

**Joshi, C.P.** (1987a). An inspection of the domain between putative TATA box and translation start site in 79 plant genes. Nucl. Acids Res. **15,** 6643–6653.

**Joshi, C.P.** (1987b). Putative polyadenylation signals in nuclear genes of nuclear genes of higher plants: A compilation and analysis. Nucl. Acids Res. **15,** 9627–9639.

**Klein, T.M., Wolf, E.D., Wu, R., and Sanford, J.C.** (1987). High-

velocity microprojectiles for delivering nucleic acids into living cells. Nature **327,** 70–73.

**Klein, T.M., Gradziel, T., Fromm, M.E., and Sanford, J.C.** (1988). Factors influencing gene delivery into *Zea mays* cells by high-velocity microprojectiles. Bio/Technology **6,** 559–563.

**Klein, T.M., Roth, B.A., and Fromm, M.E.** (1989). Regulation of anthocyanin biosynthetic genes introduced into intact maize tissues by microprojectiles. Proc. Natl. Acad. Sci. USA **86,** 6681–6685.

**Kozak, M.** (1984). Selection of initiation sites by eucaryotic ribosomes: Effect of inserting AUG triplets upstream from the coding sequence for preproinsulin. Nucl. Acids Res. **12,** 3873–3893.

**Krieg, P.A., and Melton, D.A.** (1987). In vitro RNA synthesis with SP6 RNA polymerase. Methods Enzymol. **155,** 397–415.

**Logemann, J., Schell, J., and Willmitzer, L.** (1987). Improved method for the isolation of RNA from plant tissues. Anal. Biochem. **163,** 16–20.

**Luehrsen, K.R., and Walbot, V.** (1991). Intron enhancement of gene expression and the splicing efficiency of introns in maize cells. Mol. Gen. Genet., in press.

**McCarty, D.R., Carson, C.B., Lazar, M., and Simonds, S.C.** (1989). Transposable element-induced mutations of the *viviparous-1* gene in maize. Dev. Genet. **10,** 473–481.

**McLaughlin, M., and Walbot, V.** (1987). Cloning of a mutable *bz2* allele of maize by transposon tagging and differential hybridization. Genetics **117,** 771–776.

**Ortiz, D.F., and Strommer, J.N.** (1990). The *Mu1* maize transposable element induces tissue-specific aberrant splicing and polyadenylation in two *Adh1* mutants. Mol. Cell. Biol. **10,** 2090–2095.

**Reddy, G.M., and Coe, E.H., Jr.** (1962). Inter-tissue complementation: A simple technique for direct analysis of gene action sequence. Science **138,** 149–150.

**Robertson, D.S.** (1978). Characterization of a *Mutator* system in maize. Mutat. Res. **51,** 21–28.

**Sambrook, J., Fritsch, E.F., and Maniatis, T.** (1989). Molecular Cloning: A Laboratory Manual. (Cold Spring Harbor, NY: Cold Spring Harbor Laboratory).

**Schmidt, R.J., Burr, F.A., and Burr, B.** (1987). Transposon-tagging and molecular analysis of the maize regulatory locus *opaque-2*. Science **238,** 960–963.

**Strommer, J., and Ortiz, D.** (1989). *Mu1*-induced mutant alleles of maize exhibit background-dependent changes in expression and RNA processing. Dev. Genet. **10,** 452–459.

**Taylor, L.P., and Briggs, W.R.** (1990). Genetic regulation and photocontrol of anthocyanin accumulation in maize seedlings. Plant Cell **2,** 115–127.

**Theres, N., Scheele, T., and Starlinger, P.** (1987). Cloning of the *Bz2* locus of *Zea mays* using the transposable element *Ds* as a gene tag. Mol. Gen. Genet. **209,** 193–197.

**Theres, N., Schmitz, G., Scheele, T., and Starlinger, P.** (1988). The *Bz2* locus in maize: Cloning and transcription studies. In The Genetics of Flavonoids, G.A. Gavazzi, M.L. Racchi, and D.E. Styles, eds (Victoria, British Columbia, Canada: Edizioni Unicopli), pp. 97–104.

**Tindall, K.R., and Kunkel, T.A.** (1988). Fidelity of DNA synthesis by the *Thermus aquaticus* DNA polymerase. Biochemistry **27,** 6008–6013.

**Walbot, V., and Warren, C.** (1988). Regulation of *Mu* element copy number in maize lines with an active or inactive transposable element system. Mol. Gen. Genet. **211,** 27–34.

**Walbot, V., Britt, A.B., Luehrsen, K.R., McLaughlin, M., and Warren, C.A.** (1988). Regulation of *Mutator* activities in maize. In Plant Transposable Elements, O.E. Nelson, Jr., ed (New York: Plenum Press), pp. 121–135.

**Winter, J., Wright, R., Duck, N., Gasser, C., Fraley, R., and Shah, D.** (1988). The inhibition of petunia *hsp70* mRNA processing during $CdCl_2$ stress. Mol. Gen. Genet. **211,** 315–319.

**Yost, H.J., and Lindquist, S.** (1988). Translation of unspliced transcripts after heat shock. Science **242,** 1544–1548.